Proceedings of the National Conference on Computational Modeling of Fluid Dynamics Problems (CMFDP-2019)
NIT Warangal, India – Jan 18-20, 2019
Paper No. XXX (The number assigned when the papaer is accepted)

Mixed Convection Micropolar Nanofluid Flow in a Porous Channel: Entropy Generation Analysis

Surender Ontela [a,*], *Lalrinpuia Tlau* [a]
[a] *Department of Mathematics, National Institute of Technology Mizoram, Aizawl - 796012, Mizoram, India*
*Corresponding Author Email: reddysurender3@gmail.com

The problem of mixed convection micropolar nanofluid flow in a vertical parallel plate channel filled with a porous medium has been investigated. The equations governing momentum, microrotation and energy are non-dimensionalized and then solved using Homotopy Analysis Method (HAM). The expressions for the velocity, temperature and microrotation profiles are thus obtained. Entropy generation rate is calculated along with the irreversibility ratio. Influence of pertinent flow parameters on entropy generation and irreversibility are shown graphically and deliberated.

Keywords: Mixed Convection, Entropy, Micropolar Nanofluid, Porous Medium

1. Introduction

Nanofluids are fluids with suspended nanoparticles of the order of 1 -100 nm in it. The base fluids used are usually water, mineral oil, ethylene glycol, etc. while the nanoparticles used are usually silver, titanium, copper, and alumina. Since Choi[1] coined the term 'Nanofluids', the field has advanced rapidly in the proceeding years. Academicians and industrialists alike have taken a yearning interest to advance the field in theory and in applications. Nanofluids have been found to increase the heat transfer capacity of fluids. General applications of nanofluids have been reviewed in the articles[2 – 5].

Eringen[6] introduced the theory of micropolar fluids considering fluids with micro-rotational effects and micorotational inertia. Micopolar fluids are fluids which comprise of rigid, randomly oriented or spherical particles with their own spins and rotations. Animal blood, ferrofluids, liquid crystals are some examples of fluids in this category. Chamkha et.al[7] studied a free convection flow in a vertical channel, and concluded that an increase in the temperature ratio of the walls increases the temperature and velocity profiles, respectively. Chamkha et. al[8] concluded that for a mixed convective flow in a vertical channel, the temperature and velocity profiles can become highly distorted in developing regions. Cheng [9] obtained analytical results for free convection heat and mass transfer of a micropolar fluid in a vertical channel with asymmetric wall temperatures and concentrations and also studied the effects of vortex viscosity parameter and the buoyancy ratio, while Bataineh et.al[10] studied the same problem using HAM. Abdulaziz et.al [11] also used HAM to study heat transfer in micropolar fluid flow and showed that magnetic field and micropolar effects are useful in reducing heating effects and in controlling the rate of heat transfer. Kumar et.al[12] showed that micropolar fluids act as cooling agents and also reduce drags on the walls of the flow surface. Ashmawy[13] studied a fully developed natural convective flow considering effects of slip conditions.

Micropolar nanofluids are micropolar fluids with nanoparticles added in them. Mohyud-Din et.al.[14] studied magnetohydrodynamic(MHD) flow in a porous channel with radiation effects. Hussain et.al[15] concluded that an increase in the nanoparticle volume fraction causes Nusselt number to decline while it increased the velocity and temperature profiles, respectively. Turk and Tezer-Sezgin[16] were the first to use FEM to solve highly nonlinear governing equations of micropolar nanofluid flow. Haq et al.[17] proposed a mathematical model for natural convective micropolar nanofluid flow. Noor et al.[18] studied stagnation flow of micropolar nanofluids and the effects of slip on the heat transfer rate.

Entropy generation and heat transfer phenomenon are linked and must be studied simultaneously. Bejan[19] conducted a pioneering study of entropy generation in convective heat transfer phenomena. Srinivasacharya and Bindu[20] studied the entropy generation in a micropolar flow in an inclined channel. Srinivas et.al [21] used HAM to solve the problem of flow of two immiscible micropolar fluids, and showed that irreversibility was minimized at the interface of the two fluids. Srinivasacharya and Bindu[22] studied flow of micropolar fluid in a pipe with convective boundary conditions and showed that entropy rate decrease with increase in Biot number. Khan et.al[23] studied the slip effects for flow in a rotating disk and showed that entropy generation could be controlled and decreased using slip. Srinivas et.al[24] studied the effects of radiation for flow in a non-Darcian porous medium and observed that increasing radiation increased entropy in the flow.

Literature on micropolar nanofluids is still very limited. The present study deals with the mixed convection micropolar nanofluid flow in a vertical channel filled with a porous medium. The mathematical model of mixed convection micropolar nanofluid constitutes a system of coupled ordinary differential equations. The non-dimensionalized governing equations are solved using HAM proposed by Liao[25]. The influence of significant parameters on entropy generation and Bejan number are presented graphically and deliberated.

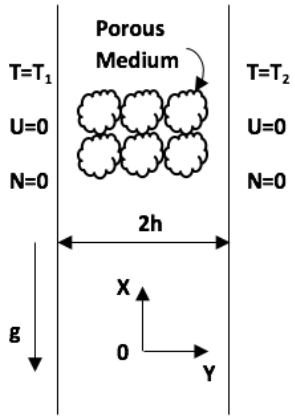

Figure. 1: Schematic diagram with coordinates axes

2. Mathematical Formulation

Consider a mixed convection micropolar nanofluid flow in a vertical channel filled with a porous medium as shown in Fig.1. The x - coordinate is taken along the plate and the y - coordinate is taken normal to the plate. The walls of the channel are assumed to be heated uniformly but at different temperature, with the left wall at T_1 and right wall at T_2 ($T_2 > T_1$). The governing equations can thus be written as

$$(\mu_{nf} + \kappa)\frac{d^2u}{dy^2} + \kappa\frac{dn}{dy} + g(\rho\beta)_{nf}(T - T_0) - \frac{dp}{dx} - \frac{\mu_{nf}}{K}u = 0, \quad (1)$$

$$\gamma\frac{d^2n}{dy^2} - \kappa\left(2n + \frac{du}{dy}\right) = 0, \quad (2)$$

$$\frac{d^2T}{dy^2} = 0, \quad (3)$$

subject to the boundary conditions:

$$u(-h) = 0,\ T(-h) = T_1,\ n(-h) = 0, \quad (4a)$$

$$u(h) = 0,\ T(h) = T_2,\ n(h) = 0, \quad (4b)$$

where u is the axial velocity, T is the fluid temperature, n is the microrotation component of the

micropolar fluid normal to the (x; y) - plane, subscript nf is the nanofluid component, ρ_{nf} is the density, β_{nf} is the coefficient of thermal expansion, g is the gravitational acceleration, μ_{nf} is the dynamic viscosity, κ is the vortex viscosity, K is permeability of the porous medium and γ is the spin gradient viscosity.

Introducing the following non-dimensional variables

$$X = \frac{x}{h},\ Y = \frac{y}{h},\ U = \frac{u}{U_0},\ \theta = \frac{T-T_1}{T_2-T_1},\ N = \frac{h}{U_0}n,\ \overline{P} = \frac{p}{\rho_f U_0^2}, \tag{5}$$

where U_0 is the characteristic velocity, into Eqs (1)-(3), we get

$$[A_1 + c]\frac{d^2U}{dY^2} + c\frac{dN}{dY} + A_2\frac{Gr}{Re}\theta - ReP - A_1\frac{U}{Da} = 0, \tag{6}$$

$$\frac{d^2N}{dY^2} - s\left(2N + \frac{dU}{dY}\right) = 0, \tag{7}$$

$$\frac{d^2\theta}{dY^2} = 0, \tag{8}$$

where $c = \frac{\kappa}{\mu_f}$ is micropolarity parameter, $Gr = \frac{\rho_f^2\beta_f g h^3(T_2-T_1)}{\mu_f^2}$ is Grashof number, $Re = \frac{\rho_f U_0 h}{\mu_f}$ is Reynolds number, $Br = \frac{U_0\mu_f}{k_f(T_2-T_1)}$ is Brinkman number, $Da = \frac{K}{h^2}$ is Darcy number, $s = \frac{\kappa h^2}{\gamma}$ is couple stress parameter, $P = \frac{d\bar{P}}{dX}$ is dimensionless pressure gradient, $A_1 = \frac{1}{(1-\emptyset)^{2.5}}$, $A_2 = \left[(1-\emptyset) + \emptyset\frac{(\rho\beta)_s}{(\rho\beta)_f}\right]$ and $A_2 = \frac{k_{nf}}{k_f}$.

The associated dimensionless boundary conditions are

$$U(-1) = 0, \theta(-1) = 0, N(-1) = 0, \tag{9a}$$

$$U(1) = 0, \theta(1) = 1, N(1) = 0. \tag{9b}$$

3. Solution using HAM

We consider the auxiliary linear operators for the HAM as

$$L_i = \frac{\partial^2}{\partial Y^2}, \qquad i = 1,2 \tag{10}$$

while the initial approximations of U(Y) and N(Y) are taken as

$$U_0 = 0\ , N_0 = 0, \tag{11}$$

such that

$$L_1(c_1 + c_2Y) = 0\ , L_2(c_3 + c_4Y) = 0, \tag{12}$$

where c_i $(i = 1,2,3,4)$ are constants.

Equation (9) subject to the boundary conditions (10) has the exact solution

$$\theta = \frac{1+Y}{2}. \tag{13}$$

We introduce the non-zero auxiliary parameters h_1 and h_2 and develop the zeroth-order deformation equations as

$$(1-p)L_1[U(Y;p) - U_0(Y)] = ph_1M_1[U(Y;p)], \tag{14}$$

$$(1-p)L_2[N(Y;p) - N_0(Y)] = ph_2M_2[N(Y;p)], \tag{15}$$

subject to the boundary conditions

$$U(-1;p) = 0\ ,\ N(-1;p) = 0, \tag{16a}$$

$$U(1;p) = 0\ ,\ N(1;p) = 0, \tag{16a}$$

where $p \in [0,1]$ is the embedding parameter and the non-linear operators M_1 and M_2 are defined as

$$M_1[U(Y;p), \theta(Y;p)] = [A_1 + c]U'' + cN' + A_2\frac{Gr}{Re}\left(\frac{1+Y}{2}\right) - ReP - A_1\frac{U}{Da}, \tag{17}$$

$$M_2[U(Y;p), N(Y;p)] = N'' - s(2N + U'). \tag{18}$$

For p=0 we have the initial guess approximations

$$U(Y;0) = U_0(Y),\ N(Y;0) = N_0(Y), \tag{19}$$

and for p=1 we get the final expression

$$U(Y;1) = U(Y),\ N(Y;1) = N(Y). \tag{20}$$

Therefore, as p increases from 0 to 1, U(Y;p) and N(Y;p) varies continuously from the initial guess $U_0(Y)$ and $N_0(Y)$ to the final expressions U(Y) and N(Y), respectively. The m^{th}-order deformation equations are written as

$$L_1[U_m(Y) - \chi_m U_{m-1}(Y)] = h_1 O_m^U(Y), \tag{21}$$

$$L_2[N_m(Y) - \chi_m N_{m-1}(Y)] = h_2 O_m^N(Y), \tag{22}$$

with boundary conditions

$$U(-1) = 0,\ N(-1) = 0, \tag{23a}$$

$$U(1) = 0,\ N(1) = 0. \tag{23b}$$

And

$$O_m^U(Y) = [A_1 + c]U'' + cN' + A_2 \frac{Gr}{Re}\left(\frac{1+Y}{2}\right) - ReP - A_1 \frac{U}{Da}, \tag{24}$$

$$O_m^N(Y) = N'' - s(2N + U'), \tag{25}$$

where m is an integer and

$$\chi_m = \begin{cases} 0, & for\ m \le 1 \\ 1, & for\ m > 1 \end{cases}. \tag{26}$$

The initial approximations, linear operators and auxiliary parameters are chosen such that equations (14) - (16) have a solution at each point of $p \in [0,1]$. Using Taylor's series and equation (16), the solutions expression can be written as

$$U(Y;p) = U_0(Y) + \sum_{m=1}^{\infty} U_m(Y)p^m, \tag{27}$$

$$N(Y;p) = N_0(Y) + \sum_{m=1}^{\infty} N_m(Y)p^m, \tag{28}$$

where h_1 and h_2 are chosen such that the series (27) and (28) are convergent at p=1. Hence, we have the final expression

$$U(Y) = U_0(Y) + \sum_{m=1}^{\infty} U_m(Y), \tag{29}$$

$$N(Y) = N_0(Y) + \sum_{m=1}^{\infty} N_m(Y) \tag{30}$$

with

$$U_m(Y) = \frac{1}{m!}\frac{\partial^m U(Y;p)}{\partial p^m}\Big|_{p=1} \text{ and } N_m(Y) = \frac{1}{m!}\frac{\partial^m N(Y;p)}{\partial p^m}\Big|_{p=1} \tag{31}$$

The HAM solution is strongly dependent on the convergence control parameter h. To assure convergence of the solution expression, h-curves are plotted for various values, as shown in Fig. 2 from 14^{th} order HAM approximation. It is clear from Fig.2 that the admissible range for h_1 is $-1 \le h_1 \le -0.25$ and that for h_2 is $-1 \le h_2 \le -0.25$. To choose the optimal value of convergence control parameter, the average residual errors are defined as[26]:

$$E_{U,m} = \frac{1}{K}\sum_{i=0}^{K}\left[M_1\left(\sum_{j=0}^{m} U_k(j\Delta t)\right)\right], \tag{32}$$

$$E_{N,m} = \frac{1}{K}\sum_{i=0}^{K}\left[M_2\left(\sum_{j=0}^{m} N_k(j\Delta t)\right)\right], \tag{33}$$

where $\Delta t = 1/K$ and K=40. The minimum average residual errors are shown in Table 1 for different order approximations. Thus, the minimum average residual error for U is taken at h_1=-0.5 and for N is taken at h_2 = -0.8.

Table 1: Optimal values of h_1 and h_2 for different orders of approximation

Order(m)	h_1	Minimum error	h_2	Minimum error
10	-0.5	1.42965×10^{-6}	-0.8	4.51361×10^{-8}
12	-0.5	4.54371×10^{-7}	-0.8	1.32445×10^{-9}

14	-0.5	1.68147×10^{-7}	-0.8	4.09599×10^{-11}

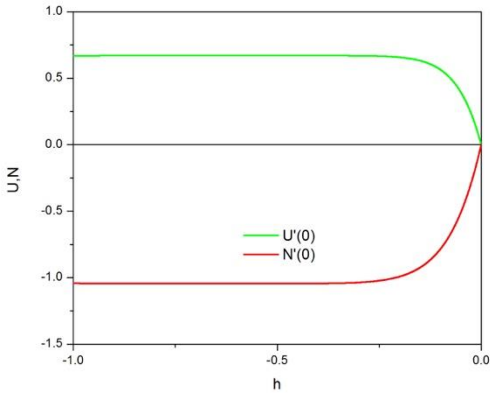

Figure 2: h curves for U'(0) and N'(0) when *c*=0.1, *Re*=0.1,*P*=1,*Gr*=1,*Da*=1,*S*=1,ø =1% from 14th order HAM approximation

4. Entropy Generation

The local volumetric rate of entropy generation S_G for a micropolar nanofluid flow in a porous medium is given by

$$S_G = \frac{k_{nf}}{T_0^2}\left(\frac{dT}{dy}\right)^2 + \frac{\mu_{nf}}{T_0}\left(\frac{du}{dy}\right)^2 + \frac{\kappa}{T_0}\left(\frac{du}{dy} + 2n\right)^2 + \frac{b}{T_0}\left(\frac{dn}{dy}\right)^2 + \frac{\mu_{nf}}{T_0 K}u^2. \quad (34)$$

The dimensionless entropy generation rate is given by $N_s = \frac{h^2 T_0^2}{k_f(T_2 - T_1)} S_G$, and using (34) we have

$$N_s = A_3\left(\frac{d\theta}{dY}\right)^2 + \frac{Br}{\Omega}\left\{A_1\left(\frac{dU}{dY}\right)^2 + c\left(\frac{dU}{dY} + 2N\right)^2 + \delta\left(\frac{dN}{dY}\right)^2 + A_1\frac{U^2}{Da}\right\}. \quad (35)$$

The first term on the right-hand side of the above equation denotes the entropy generated due to heat transfer irreversibility and the second term denotes the entropy generated due to fluid friction/viscous dissipation. To evaluate the cause of irreversibility, the Bejan number is introduced, which is a ratio of heat transfer irreversibility and total entropy generated, defined as

$$Be = \frac{N_H}{N_H + N_F}, \quad (36)$$

where $N_H = A_3\left(\frac{d\theta}{dY}\right)^2$ and $N_F = \frac{Br}{\Omega}\left\{A_1\left(\frac{dU}{dY}\right)^2 + c\left(\frac{dU}{dY} + 2N\right)^2 + \delta\left(\frac{dN}{dY}\right)^2 + A_1\frac{U^2}{Da}\right\}$.

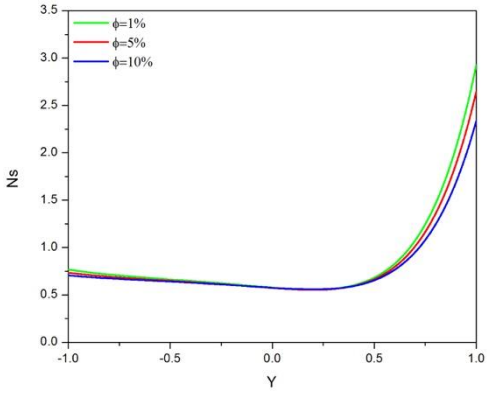

Figure 3: Effect of ∅ on Entropy generation rate

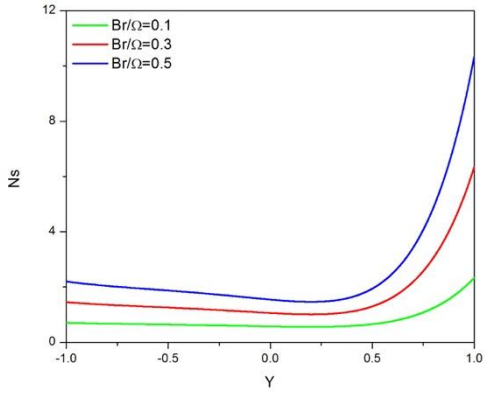

Figure 4: Effect of Br/Ω on Entropy generation rate

The Bejan number varies from 0 to 1. For $Be \approx 0$, the irreversibility is completely dominated by fluid friction irreversibility. For $Be \approx 1$, the irreversibility is completely dominated by heat transfer irreversibility. At $Be = 0.5$, the contribution of fluid friction irreversibility and heat transfer irreversibility are equal.

5. Results and Discussions

The solutions for velocity and microrotation profiles have been calculated using the homotopy analysis method. Along with the expression for temperature, the entropy generation rate and irreversibility ratio have been calculated.

The influence of nanoparticle volume fraction on the entropy generation rate is shown in fig. 3. An overall decrease in entropy generation rate is seen with increase in nanoparticle volume fraction. The decrease is more prominent as we get closer to the right wall of the channel. Fig 4. shows the influence of the dimensionless parameter,Br/Ω (ratio of Brinkman number and temperature difference ratio). This dimensionless number has an increasing influence in the entropy generation due to increase in viscous dissipation. Increase in the mixed convection parameter *Gr/Re* and its effect on the entropy generation rate can be seen in fig 5. The mixed convection parameter causes a significant increase in the entropy generation rate. It may also be noted that this increase in entropy increases more significantly along the right wall of the channel. The micropolarity parameter *c* has a decreasing effect on the entropy generation rate, as shown in fig 6. It may be noted that the rate of entropy generation is higher near the right wall of the channel for all cases.

The entropy generation rate fails to convey whether the entropy generated is dominated by heat transfer or fluid friction/viscous dissipation. On this note, the Bejan number is examined so as to ascertain the aforementioned dilemma. Fig 7 shows the influence of increasing nanoparticle volume fraction on the Bejan number. Addition of more nanoparticles to the fluid causes an increase in Bejan number, which depicts the increasing dominance of heat transfer irreversibility. The influence of the dimensionless parameter Br/Ω on Bejan number can be seen in fig 8. Br/Ω causes the Bejan number to decrease significantly. This is because viscous dissipation increases with increasing Br/Ω. For low values of *Gr/Re*, it may be observed that Bejan number is closer to 1, as shown in fig 9. The Bejan number drops significantly as *Gr/Re* is increased, and more so near the right wall of the channel. The increase in micropolarity parameter *c* causes an increase in the Bejan number, as shown in fig 10. For all cases, it may be noted that Bejan number is lowest near the right wall of the channel.

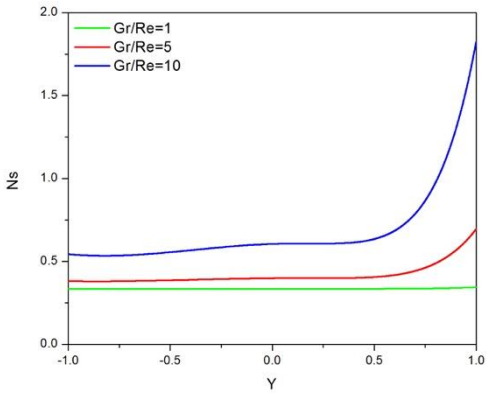

Figure 5: Influence of *Gr/Re* on Entropy generation rate

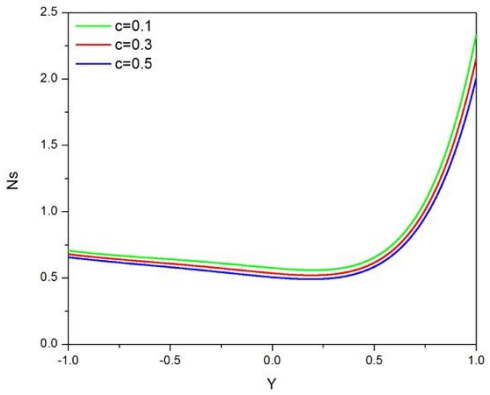

Figure 6: Influence of *c* on Entropy generation rate

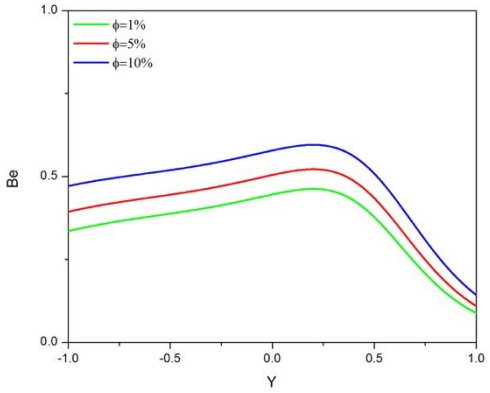

Figure 7: Effect of ∅ on Bejan number

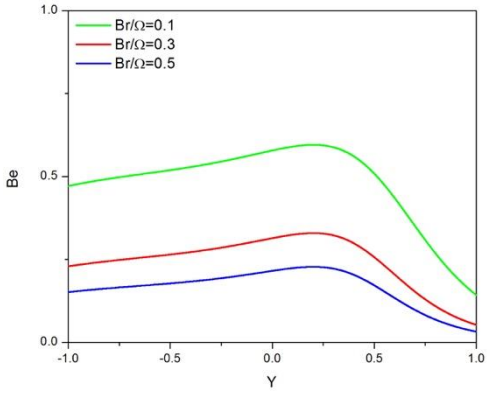

Figure 8: Effect of Br/Ω on Bejan number

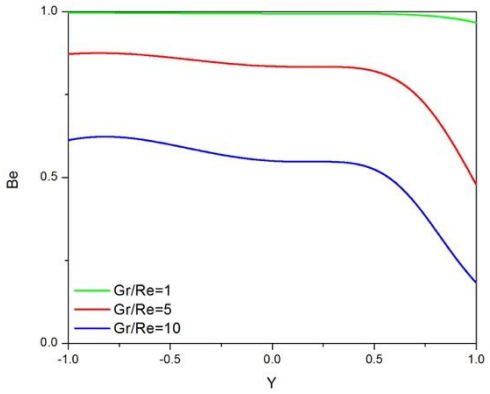

Figure 9: Influence of *Gr/Re* on Bejan number

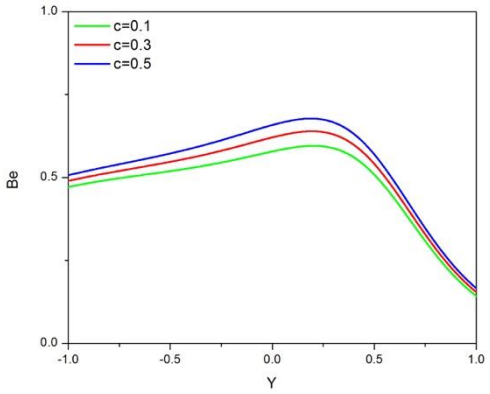

Figure 10: Influence of *c* on Bejan number

6. Conclusions

In this article, the problem of a mixed convection micropolar nanofluid flow in a vertical channel filled with a porous medium has been solved. The homotopy analysis method was used to tackle the problem. The following conclusions are made from our analysis:

- The increase in nanoparticle volume fraction causes entropy generation rate to decrease slightly while there was a prominent increase in Bejan number.
- There was a significant increase in entropy generation rate while Bejan number decreased with increase in Br/Ω.
- An increase in mixed convection parameter augments entropy generation rate while Bejan number decreased for the same.

References:

[1] S. U. S. Choi and J. A. Eastman, "Enhancing thermal conductivity of fluids with nanoparticles," *ASME Int. Mech. Eng. Congr. Expo.*, vol. 66, no. March, pp. 99–105, 1995.

[2] K. V. Wong and O. De Leon, "Applications of nanofluids: Current and future," *Adv. Mech. Eng.*, vol. 2010, 2010.

[3] R. Saidur, K. Y. Leong, and H. A. Mohammad, "A review on applications and challenges of nanofluids," *Renew. Sustain. Energy Rev.*, vol. 15, no. 3, pp. 1646–1668, 2011.

[4] A. K. Sharma, A. K. Tiwari, and A. R. Dixit, "Progress of Nanofluid Application in Machining: A Review," *Mater. Manuf. Process.*, vol. 30, no. 7, pp. 813–828, 2015.

[5] S. K. Verma and A. K. Tiwari, "Progress of nanofluid application in solar collectors: A review," *Energy Convers. Manag.*, vol. 100, pp. 324–346, 2015.

[6] A. C. Eringen, "Theory of Micropolar Fluids," *J. Math.Mech.*, vol. 16, no. 1, pp. 1–18, 1966.

[7] A. J. Chamkha, T. Grosan, and I. Pop, "Fully developed free convection of a micropolar fluid in a vertical channel," *Int. Commun. Heat Mass Transf.*, vol. 29, no. 8, pp. 1119–1127, 2002.

[8] A. J. Chamkha, T. Grosan, and I. Pop, "Fully Developed Mixed Convection of a Micropolar Fluid in a Vertical Channel," *Int. J. Fluid Mech. Res.*, vol. 30, no. 3, pp. 251–263, Nov. 2003.

[9] C. Y. Cheng, "Fully developed natural convection heat and mass transfer of a micropolar fluid in a vertical channel with asymmetric wall temperatures and concentrations," *Int. Commun. Heat Mass Transf.*, vol. 33, no. 5, pp. 627–635, 2006.

[10] T. E. Tezduyar, S. Sathe, M. Schwaab, and B. S. Conklin, "Arterial fluid mechanics modeling with the stabilized space – time fluid – structure interaction technique," *Int. J. Numer. Methods Fluids*, vol. 2006, no. October 2007, pp. 601–629, 2008.

[11] O. Abdulaziz, N. F. M. Noor, and I. Hashim, "Homotopy analysis method for fully developed MHD micropolar fluid flow between vertical porous plates," *Int. J. Numer. Methods Eng.*, vol. 78, no. 7, pp. 817–827, May 2009.

[12] L. Kumar, R. Bhargava, P. Bhargava, and H. S. Takhar, "Finite element solution of mixed convection micropolar fluid flow between two vertical plates with varying temperature," pp. 251–264, 2005.

[13] E. A. Ashmawy, "Fully developed natural convective micropolar fluid flow in a vertical channel with slip," *J. Egypt. Math. Soc.*, vol. 23, no. 3, pp. 563–567, 2015.

[14] S. T. Mohyud-Din, S. U. Jan, U. Khan, and N. Ahmed, "MHD flow of radiative micropolar nanofluid in a porous channel: optimal and numerical solutions," *Neural Comput. Appl.*, vol. 29, no. 3, pp. 793–801, 2018.

[15] S. T. Hussain, S. Nadeem, and R. Ul Haq, "Model-based analysis of micropolar nanofluid flow over a stretching surface," *Eur. Phys. J. Plus*, vol. 129, no. 8, 2014.

[16] Türk and M. Tezer-Sezgin, "FEM solution to natural convection flow of a micropolar nanofluid in the presence of a magnetic field," *Meccanica*, vol. 52, no. 4–5, pp. 889–901, 2017.

[17] U. Rizwan, S. Nadeem, N. S. Akhbar, and Z. H. Khan, "Buoyancy and Radiation Effect on Stagnation Point Flow of Micropolar Nanofluid Along a Vertically," *IEEE Trans. Nanotechnol.*,

vol. 14, no. 1, pp. 42–50, 2015.

[18] N. F. M. Noor, R. U. Haq, S. Nadeem, and I. Hashim, "Mixed convection stagnation flow of a micropolar nanofluid along a vertically stretching surface with slip effects," *Meccanica*, vol. 50, no. 8, pp. 2007–2022, 2015.

[19] A. Bejan, "A Study of Entropy Generation in Fundamental Convective Heat Transfer," *J. Heat Transfer*, vol. 101, no. 4, p. 718, 1979.

[20] D. Srinivasacharya and K. Himabindu, "Effect of slip and convective boundary conditions on entropy generation in a porous channel due to micropolar fluid flow," *Int. J. Nonlinear Sci. Numer. Simul.*, vol. 19, no. 1, pp. 11–24, 2018.

[21] J. Srinivas, J. V. R. Murthy, and A. J. Chamkha, "Analysis of entropy generation in an inclined channel flow containing two immiscible micropolar fluids using HAM," *Int. J. Numer. Methods Heat Fluid Flow*, vol. 26, no. 3–4, pp. 1027–1049, 2016.

[22] D. Srinivasacharya and K. Himabindu, "Entropy generation of micropolar fluid flow in an inclined porous pipe," *Adv. Appl. Fluid Mech.*, vol. 20, no. 3, pp. 335–351, 2017.

[23] N. A. Khan, F. Naz, and F. Sultan, "Entropy generation analysis and effects of slip conditions on micropolar fluid flow due to a rotating disk," *Open Eng.*, vol. 7, no. 1, pp. 185–198, 2017.

[24] S. Jangili, S. O. Adesanya, J. A. Falade, and N. Gajjela, "Entropy Generation Analysis for a Radiative Micropolar Fluid Flow Through a Vertical Channel Saturated with Non-Darcian Porous Medium," *Int. J. Appl. Comput. Math.*, vol. 3, no. 4, pp. 3759–3782, 2017.

[25] S. Liao, *Beyond Perturbation: Homotopy*, vol. 2, no. 5. Chapman and Hall/CRC, 2004.

[26] S. Liao, "An optimal homotopy-analysis approach for strongly nonlinear differential equations," *Commun. Nonlinear Sci. Numer. Simul.*, vol. 15, no. 8, pp. 2003–2016, 2010.